BŞEÜ Fen Bilimleri Dergisi
8(1), 413-429, 2021

BSEU Journal of Science
https://doi.org/10.35193/bseufbd.949225

e-ISSN: 2458-7575 (https://dergipark.org.tr/tr/pub/bseufbd)

Araştırma Makalesi – Research Article

Determination of Stress and Deformation Zones of Historical Mus Murat Bridge

Tarihi Muş Murat Köprüsü Gerilme ve Deformasyon Bölgelerinin Belirlenmesi

Aylin Özodabaş[1*], Cüneyt Artan[2]

Geliş / Received: 07/06/2021 ***Revize / Revised: 12/06/2021*** ***Kabul / Accepted: 14/06/2021***

ABSTRACT

This study was carried out to determine the strength of long span stone bridges and stress areas of a historical bridge by using finite element method during earthquakes, floods, and vehicle traffic. The possible earthquake impact of the region and the behavior of the bridge under the effect of the 2011 Van earthquake were investigated. The stresses that will be caused by hydrostatic and vehicle loading applied to the bridge are dwelled on. This study aimed to shed light on future restoration work. As a result of the vehicle, hydrostatic load and dead load analysis, the biggest deformation occurred in the arch K9, which has the largest arch span. According to the results of the earthquake analysis, maximum deformation occurred in the K10 arch, which is one of the arches with the largest arch span of the bridge. In addition, inearthquakes affected in the X and Z direction, it was observed that the arches and piers in the middle of the bridge, that is, these relatively higher structural elements were subjected to more stress. It has been determined that the A11 pier of the bridge is the structural element exposed to the most pressure.

Keywords- Historical Bridges, Finite Elements, Linear Analysis

ÖZET

Depremler, seller ve araç trafiği sırasında uzun açıklıklı taş köprülerin dayanımını ve tarihi bir köprünün stres bölgelerini sonlu elemanlar yöntemi ile belirlemek için bu çalışma yapılmıştır. Bölgenin olası deprem etkisi ve 2011 Van deprem etkisi altında köprünün davranışı incelenmiştir. Köprüye taşıt yüklemesi ve hidrostatik yükleme yapılıp bu yüklemelerin oluşturacağı gerilmeler üzerinde durulmuştur. Gelecekte yapılabilecek restorasyon çalışmalarına ışık tutulması hedeflenmektedir. Yapılan taşıt, hidrostatik yük ve ölü yük analizleri sonucunda en büyük deformasyon, en büyük kemer açıklığına sahip olan K9 kemerinde meydana gelmiştir. Deprem analiz sonuçlarına göre, köprünün en geniş kemer açıklığına sahip kemerlerden biri olan K10 kemerinde maksimum deformasyon oluşmuştur. Ayrıca X ve Z doğrultusunda etki ettirilen depremlerde köprünün ortasındaki kemer ve ayakların; nispeten daha yüksek olan bu yapı elemanlarının daha fazla gerilmeye maruz kaldığı görülmüştür. Köprünün A11 ayağının en çok basınca maruz kalan yapı elemanı olduğu saptanmıştır.

Anahtar Kelimeler- Tarihi Köprüler, Sonlu Elemanlar, Lineer Analiz

[1]*Sorumlu yazar iletişim: aylin.ozodabas@bilecik.edu.tr (https://orcid.org/ 0000-0002-6011-980X)
İnşaat Mühendisliği Bölümü, Bilecik Şeyh Edebali Üniversitesi, Mühendislik Fakültesi, Bilecik, Türkiye
[2]İletişim: madccproje@gmail.com (https://orcid.org/ 0000-0001-9902-9708)
İnşaat Mühendisliği Bölümü, Bilecik Şeyh Edebali Üniversitesi, Lisansüstü Eğitim Enstitüsü, Yüksek Lisans, Bilecik, Türkiye

I. INTRODUCTION

As people adopted settled life, they began to build small passageways to provide access to their certain location. Over time, due to the increase in population and the expansion of residential areas, they developed trade routes to transport the products they make to other settlements and to ensure the transportation of the products found in other settlements to their own regions. They started to build crossings (bridges) to overcome the obstacles on the route of these trade routes. In this sense, bridges have been used as a medium that connects people together for centuries.

Various structures have been built on water passages from past to present for accessibility of transportation. These structures built in the past have generally been masonry structures or bridges with wooden bases and stone piers. Technology of the period that the structures could be built with, a crossing was made with short span arch, even in rivers with very large width. Although the materials and construction techniques that are used today have changed, bridges were built in line with corresponding requirements. Today, wider watercourse spans have been crossed with fewer bridge piers and larger beam spans. Today, the emphasis is on reinforced concrete and steel bridges obtained with modern and technical materials. However, bridges built with stone materials in ancient times are of great importance [1-4].

Numerous studies have been carried out on historical arch bridges up to the present. Most of these studies have focused on examining the structural behavior of the arch form and the arch bridge. Bridges, which were analyzed with simple approaches in the past, have begun to be evaluated using more comprehensive analysis methods with the development of technology, thanks to computer software. Many experimental studies have also been carried out to investigate the applicability of these analysis methods. In recent years, it has been aimed to get closer to the actual behavior by transferring the experimental data taken on real bridges to numerical analysis [5-13]. In order to determine the stress points of the historic Mus Murat Bridge under certain loads, analysis was performed with a finite element method. Many analysis programs are available to perform structural analysis and determine the structural condition of a building. The analyzes made in this study were performed with the help of ANSYS program [14].

A. Previous Studies

Simos et al. (2018), investigated the effects of earthquakes in distant and near regions according to the location of long span historical bridges in their study. The Konitsa Bridge was chosen as an example and four earthquake parameters in that region were activated. The structure was analyzed nonlinearly and it was found that earthquakes distant from the structure are much more destructive than earthquakes nearby [15].

Chen et al. (2020), Guyue Bridge has been discussed in the study and the wear degree and mechanical properties of the bridge are tried to be determined by ultrasonic CT. It is concluded that the stress effect in historical structure; causes deformation and breakage of the stones and the atmospheric factor decreases the resistance against abrasion and evidently increases the wear rate [16].

Castro et al. (2018), conducted terrestrial laser scanner, ambient vibration tests and minor destructive tests to characterize an early reinforced concrete bridge in Portugal. These tests were carried out after the finite element model was generated. After a series of analyzes the stress points of the bridge were determined [17].

Tanrıverdi (2019), arch and bridge arches are discussed in Tanrıverdi's master's thesis. Tanrıverdi investigated the historical changes of the arches and the different materials used, and examined the advantages and disadvantages of the arches. Finally, Tanrıverdi approached to the Carpıran Bridge in Siirt and modeled the structure with the finite element method in the SAP2000 program. The self-load and earthquake behavior of the bridge were analyzed using the linear elastic analysis method [18].

Arede et al. (2019), conducted a study on determining the mechanical properties of materials used in historical masonry structures. They ran a series of tests with the samples they took on-site from the Monastery of Serra do Pilar and D. Zameiro, Lagoncinha, Vila Fria Bridges in Porto, Portugal. They attempt to determine the mechanical characterizations of the materials used in historical masonry structures with their tests [19].

BŞEÜ Fen Bilimleri Dergisi
8(1), 413-429, 2021

BSEU Journal of Science
https://doi.org/10.35193/bseufbd.949225

e-ISSN: 2458-7575 (https://dergipark.org.tr/tr/pub/bseufbd)

II. HISTORICAL MURAT BRIDGE

The Murat Bridge is located in the province of Mus, 10 km away from the city center, on the Varto road route. The location of the historical Murat Bridge on earth is 38.8627 ° latitude 41.5125 ° longitude [20, 21].

The bridge, which was rationalized with 12 arches, is pedestrianized today. The bridge was registered by the Diyarbakır Regional Board for the Conservation of Cultural and Natural Properties in 1990 [22]. The drawings of the historical building are shown in Figures 1 and Figure 2, and its present condition is shown in Figure 3.

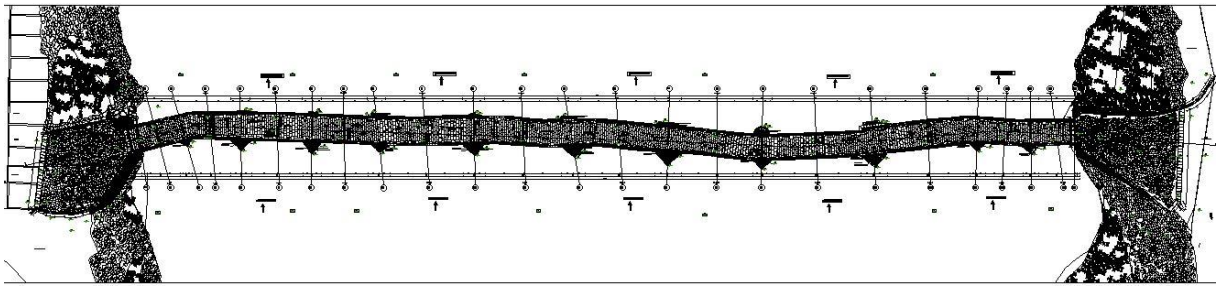


Figure 1. Historical Murat Bridge Plan View (illustrator Mehmet Sakir Guler)

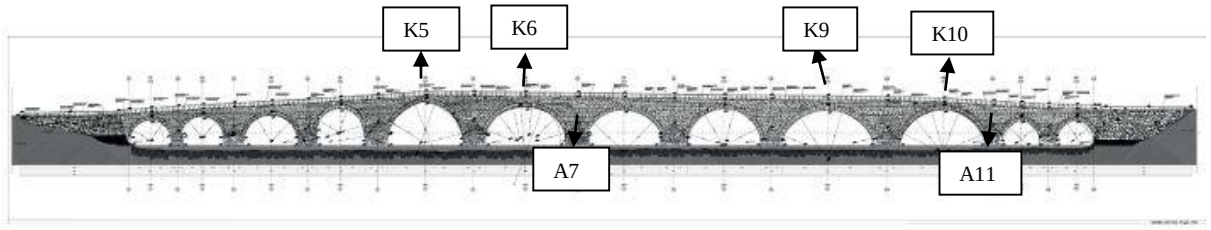


Figure 2. Historical Murat Bridge Overall View (illustrator Mehmet Sakir Guler)



Figure 3. Historical Murat Bridge Upstream View (Present Condition November 2020)

III. METHOD AND MATERIAL

The solution was reached by using the finite element method in the structural analysis. Finite element method is an essential calculation method for analyzing the statically determinate and indeterminate structural systems under various loads. Complex engineering problems contain solutions of the coequal complexity. This complexity also distracts the solution stage from acuity. The solution of complex problems in the shortest way and closest to the correct solution can be achieved by using the finite element method. Even problems that appear insoluble can be answered by this method [23]. In this study, ANSYS analysis program, which can generate solutions with finite element method, was used.

A. Analysis Method

In the finite element model, solid structures are modeled with the SOLID 185 element type. The SOLID 185 element contains 8 nodes and is a type of element that has three-dimensional linear shape functions. At each node, there are a total of 6 degrees of freedom in translation and rotation directions. The schematic of the element is shown in Figure 4 the nodes and number of elements used in the finite element model are given in Table 1.

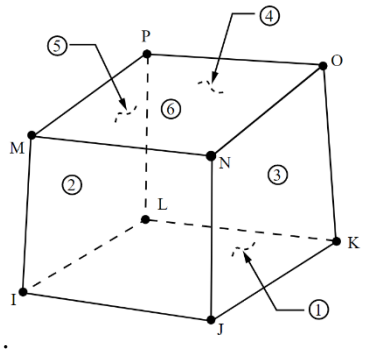


Figure 4. Schematic view of Solid 185 element

Table 1. Number of nodes and elements of the finite element model

	Node	**Element**
Model	84733	95145

The bridge geometry is meshed according to the Hex dominant method. The general view of the mesh and the bridge model are shown below in Figure 5.



Figure 5. Model and mesh display of Historical Murat Bridge

It is known that the main material used in the historical bridge is basalt stone. While doing this study, a laboratory study was not conducted on the materials used in the structure. The material properties are taken from a previous source on the historic bridge [24]. The material properties used for analysis are given in Table 2.

Table 2. Material properties accounted in the analysis of the bridge [24]

Material property	Elasticity module (N/mm^2)	Poisson ratio	Material density (kN/m^3)	Compressive Strength (MPa)
Arch stone	6960	0,3	26,2	81
Spandrel wall	6960	0,3	26,2	81

B. Analysis Performed

1. Dead-load Analysis and Modal Analysis: In accordance with the material properties entered in the ANSYS program, the analysis of the bridge was made based on the gravitational effect. The structure is modeled as a solid model. No information has been obtained about the filling material used in the building, and the filling material has been recognized and taken into account in 50% resistance of the material used in the tempered wall.

In order to obtain the free vibration behavior of the historic bridge, gravity prestressed modal analysis has been performed. 20 modes were taken into account in the analysis.

The dead-load and modal analysis model of the bridge is presented in Figure 6.

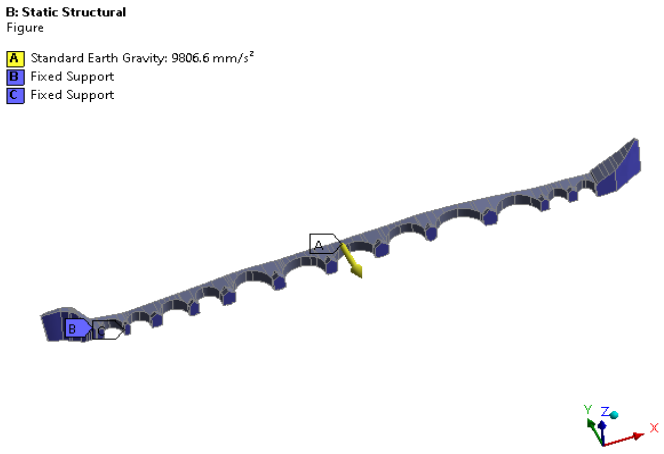


Figure 6. Model of dead-load modal analysis

2. Earthquake Analysis: In order to determine the dynamic behavior of the historic bridge, spectrum analysis was conducted. The finite element method was used for spectral analysis [25]. Earthquake analysis were made in the frequency domain.

Turkey earthquake analysis was carried out by the 2018 Turkish Building Earthquake Code ("Turkish Earthquake Code," no date) [20, 26, 27]. Since the geotechnical report required for the analysis was not available, the worst-case ground conditions were assumed. Earthquake ground motion level was taken as DD2 (50% probability of over 50 years and a repetition period of 475 years).

To determine the natural vibration periods T_A and T_B of the bridge formed during the earthquake; earthquake ground motion level (DD), soil class and the latitude/longitude of the buildings are obtained from the official website of AFAD (General Directorate of Disaster and Emergency). T_A = 0.147 s and T_B = 0.737 s. The latitude and longitude values are found at the point where the bridge is marked on the Turkey earthquake map on the AFAD's website. The acceleration spectrum graphic of the earthquake is presented in Figure 7.

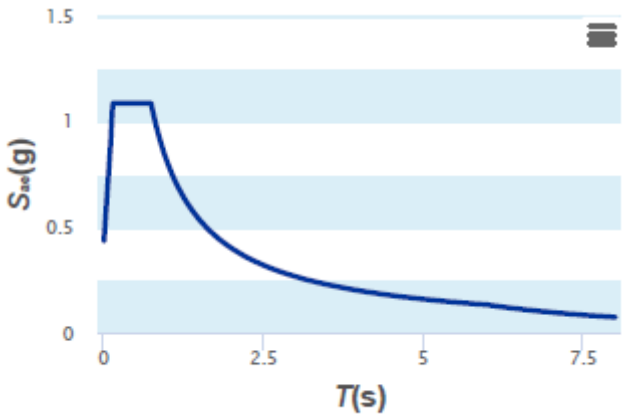


Figure 7. TBDY 2018 acceleration spectrum (period-acceleration) [20]

The data of the Van earthquake that occurred in 2011 were taken from a technical report prepared for the earthquake [28]. In Table 3, accelerometer stations measuring earthquake data are presented. One of the measurement stations, Mus Malazgirt station, is approximately 90 km away from the historical bridge. The acceleration spectrum graphic of the earthquake is presented in Figure 8.

Table 3. Maximum acceleration values measured in the van earthquake [28]

Province	District	Coordinate	NS (cm/s^2)	EW (cm/s^2)	Vertical (cm/s^2)	Distance (km)
Van	Muradiye	38.99011 43.76302	178,5	168,5	75,5	42
Muş	Malazgirt	39.14394 42.53072	44,5	25,5	95	95
Bitlis	Merkez	38.466 42.15	89,66	102,24	35,51	116
Ağrı	Merkez	39.71978 43.0164	18,45	15,08	7,21	121

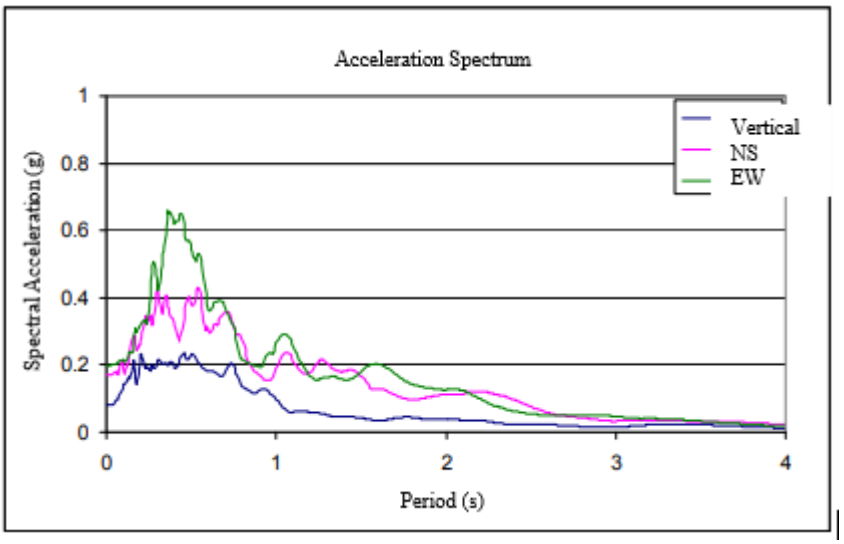


Figure 8. Van acceleration spectrum (period-acceleration) [28]

In Figure 9, the frequency acceleration graphics that are created according to the acceleration response spectra found in the earthquake data and used in the analysis are presented.

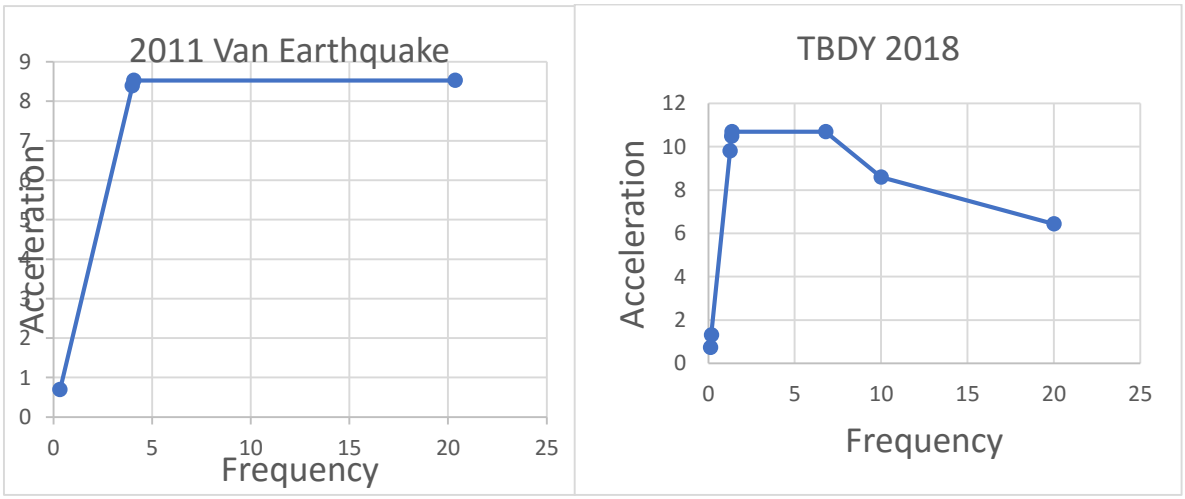


Figure 9. Earthquake data used in the analysis (frequency-acceleration)

3. Vehicle and Hydrostatic Analysis: Vehicle analysis was conducted to examine the behavior of the building under vehicle load.H30-S24 vehicles were loaded to the building with certain assumptions. H30-S24 vehicle type and axle spacing are shown in Figure 10. By choosing the minimum axle spacing, 42 vehicles were fitted to the structure and analyses were conducted under the applied pressure. Vehicle load analysis model of the building is presented in Figure 11.

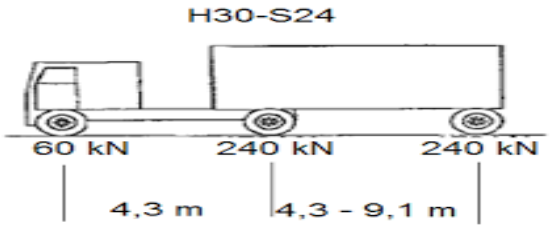


Figure 10. H30-S24 vehicle type

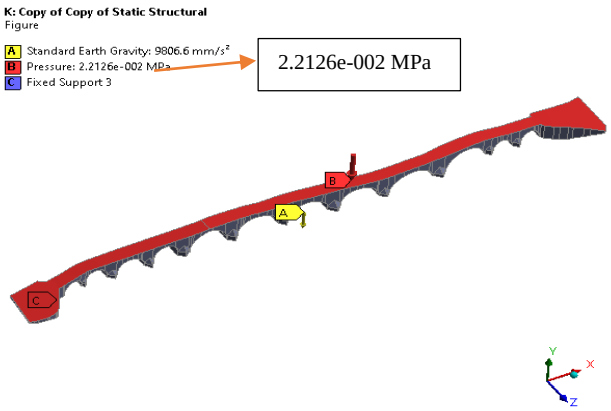


Figure 11. Model of vehicle loading analysis

The historical bridge is located on the riverbed, and there is no information available about the discharge of the river, so the hydrostatic analysis has been conducted with certain assumptions. The analysis was conducted as if there was water at the level of the bridge deck, upstream of the bridge, along the riverbed. The exerted pressure has been increased by 10% taking into account the dynamic effect of water flow. Hydrostatic pressure diagram effected on submerged areas is given in Figure 12 and hydrostatic analysis model is given in Figure 13.

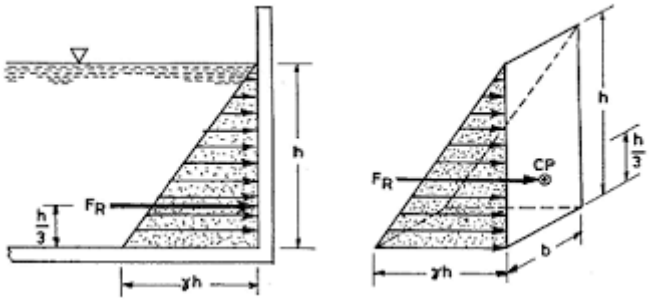


Figure 12. Hydrostatic pressure diagram effecting submerged surfaces

BŞEÜ Fen Bilimleri Dergisi
8(1), 413-429, 2021

BSEU Journal of Science
https://doi.org/10.35193/bseufbd.949225

e-ISSN: 2458-7575 (https://dergipark.org.tr/tr/pub/bseufbd)

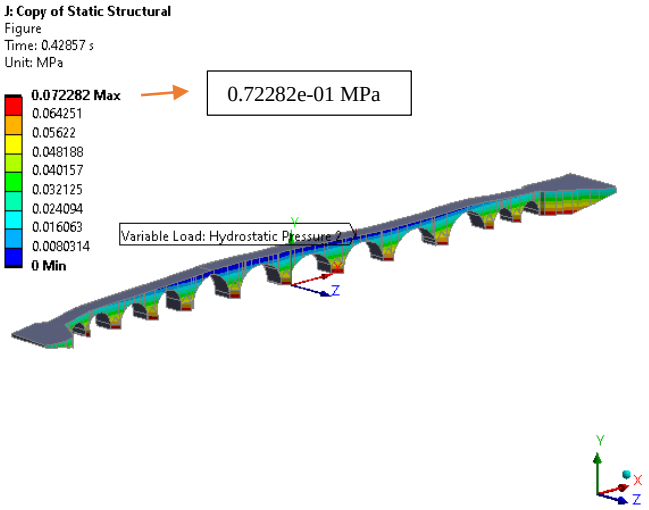


Figure 13. Hydrostatic analysis model

IV. ANALYSIS RESULTS

A. Modal Analysis

As a result of the analysis, the frequency of the structure was found in 20 modes. Frequency values occurred between 9.47 Hz and 21.73 Hz. This historical bridge is a structurally fluctuating bridge [29]. The first frequency of the bridge occurred in the K5 and K6 arches, which are higher than the other arches. The generated frequencies occurred commonly in the high and wide span (K9, K10) arches of the bridge. The natural frequencies occurring in the structure are given in Figure 14. Mass participation rates are given in Table 4.

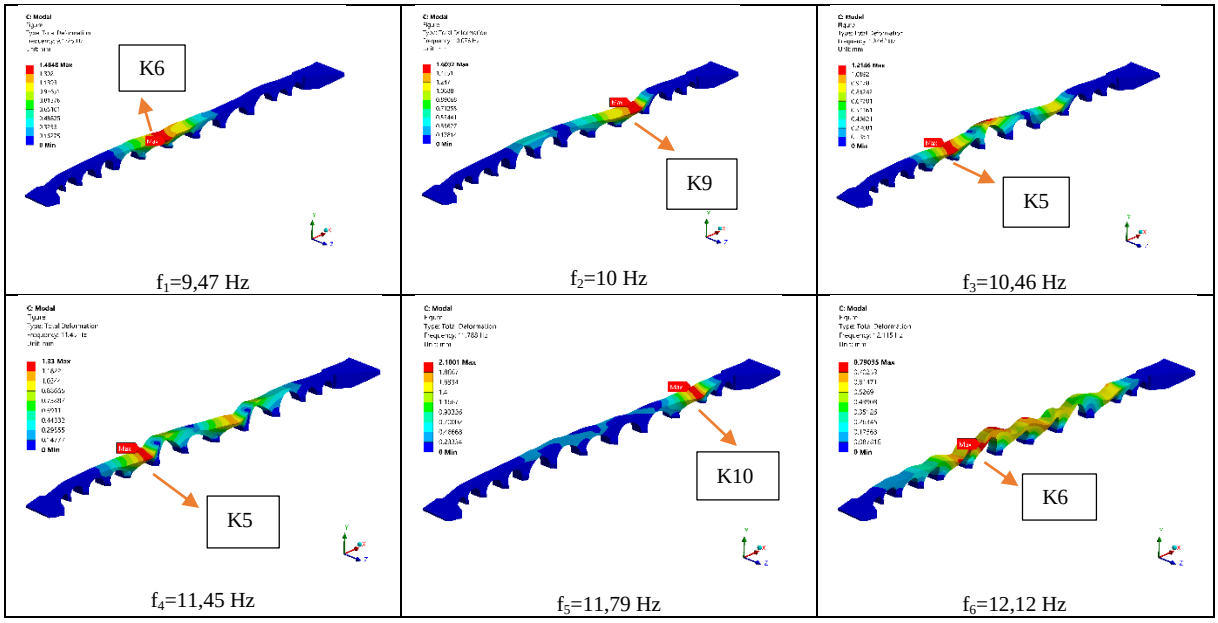
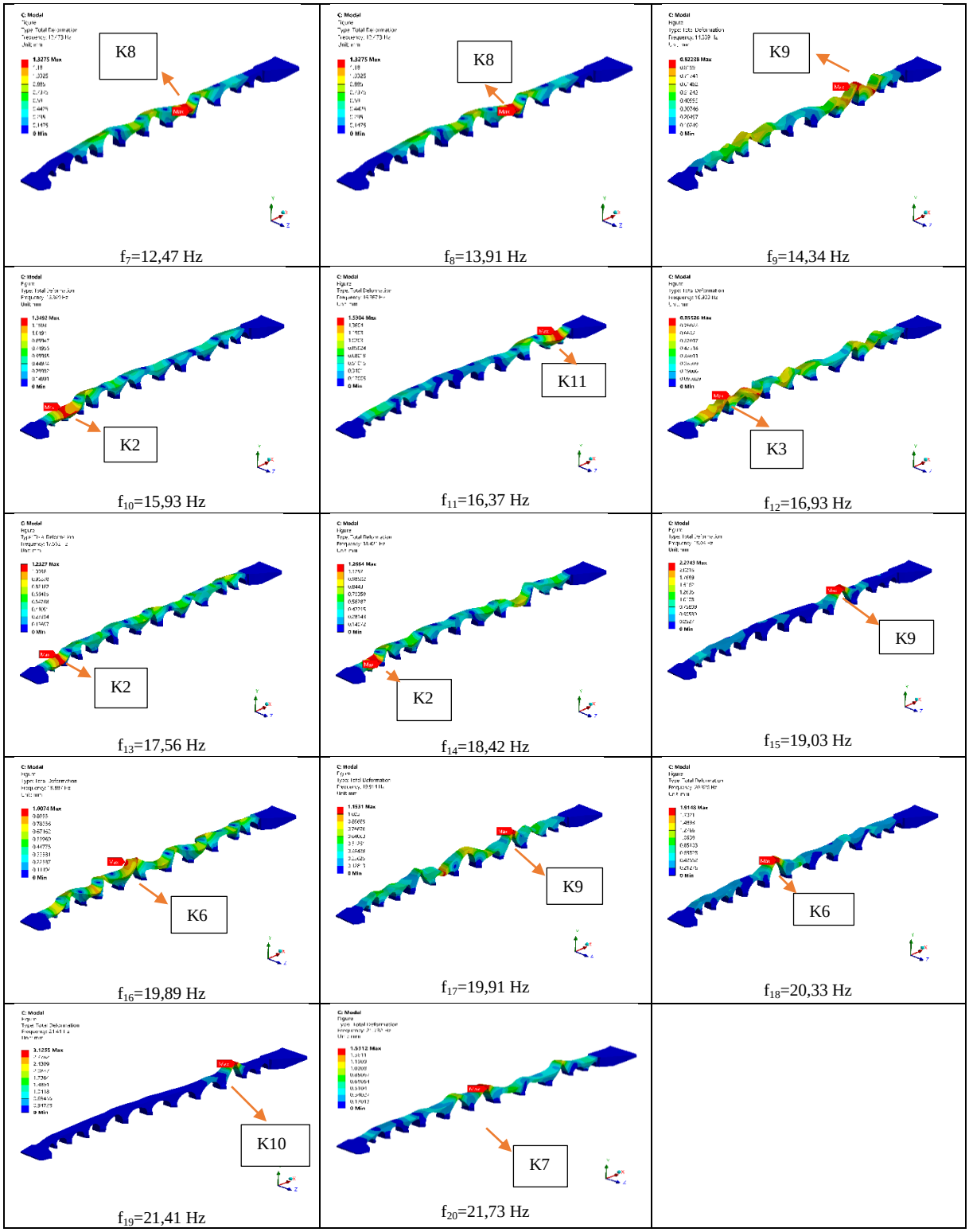


Figure 14. Natural frequencies generated on the bridge as a result of modal analysis



f_7=12,47 Hz f_8=13,91 Hz f_9=14,34 Hz

f_{10}=15,93 Hz f_{11}=16,37 Hz f_{12}=16,93 Hz

f_{13}=17,56 Hz f_{14}=18,42 Hz f_{15}=19,03 Hz

f_{16}=19,89 Hz f_{17}=19,91 Hz f_{18}=20,33 Hz

f_{19}=21,41 Hz f_{20}=21,73 Hz

Figure 14. (Continues)

Table 4. Mass participation rates as a result of modal analysis

Mode	Frequency (Hz)	Period (sn)	To Total Mass		
			X Direction	Y Direction	Z Direction
1	9.47246	0.10557	0.123139e-02	0.143175e-03	0.186868
2	10.0760	0.99245e-01	0.287793e-03	0.635984e-06	0.720014e-01
3	10.4621	0.95583e-01	0.434279e-02	0.133541e-06	0.230525e-01
4	11.4501	0.87335e-01	0.268219e-01	0.630251e-04	0.105403e-01
5	11.7880	0.84832e-01	0.322840e-01	0.130782e-03	0.762533e-01
6	12.1152	0.82541e-01	0.345620	0.644617e-05	0.166571e-01
7	12.4726	0.80176e-01	0.144311e-04	0.200159e-05	0.285677e-02
8	13.9083	0.71900e-01	0.320387e-03	0.522119e-04	0.595986e-01
9	14.3390	0.69740e-01	0.371342e-02	0.138815e-04	0.247580e-03
10	15.9293	0.62777e-01	0.133694e-02	0.505664e-04	0.852354e-02
11	16.3673	0.61097e-01	0.282693e-03	0.155448e-03	0.235701e-01
12	16.9330	0.59056e-01	0.541414e-01	0.764426e-04	0.832090e-03
13	17.5615	0.56943e-01	0.314788e-02	0.882839e-05	0.254497e-04
14	18.4212	0.54285e-01	0.104457e-02	0.110792e-02	0.202193e-01
15	19.0296	0.52550e-01	0.375999e-02	0.112405e-01	0.415688e-02
16	19.8869	0.50284e-01	0.208645e-02	0.215102e-02	0.166535e-02
17	19.9142	0.50215e-01	0.625758e-03	0.368621e-02	0.239803e-03
18	20.3259	0.49198e-01	0.552397e-03	0.769944e-02	0.815728e-04
19	21.4097	0.46708e-01	0.296683e-05	0.309358e-01	0.105638e-02
20	21.7317	0.46016e-01	0.372559e-02	0.276663e-01	0.375241e-02
Total			**0.485343**	**0.851908e-01**	**0.512198**

B. Earthquake Analysis

Earthquake data were imposed on the historical structure in three directions. The maximum deformation occurred in the 1st Mode as a result of the earthquake data impacted in the Z direction. The region of deformation that took place was occurred in the K6 arch, which is one of the highest arches of the bridge. It has been determined that earthquakes in the Z direction cause maximum stresses in the middle parts of the bridge and it has been concluded that earthquakes that will occur in this direction might cause more stress. It is seen that the earthquake effects imposed in the Y direction cause more deformation in the wide span arches (K9, K10) of the structure. Deformation in the 5th mode of the structure will be caused by the earthquakes that will occur in this direction is determined. Structurally, there is a curvature in the longitudinal direction on the historical bridge in this region. It is thought that this curvature may also cause these stresses. Considering the earthquake effect in the X direction, it is seen that it creates stress at different points. The earthquake created the maximum deformation in the 5th Mode and K10 arch of the historic bridge. At the same time, it is seen that the earthquake caused stress in the middle parts of the bridge and the highest arch, the K5. The results obtained in terms of earthquakes are presented in Figure 15

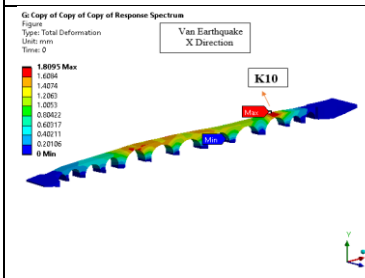
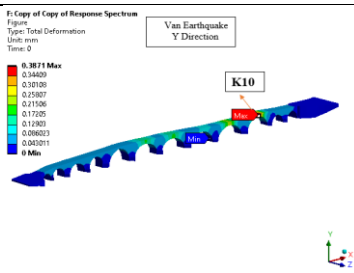
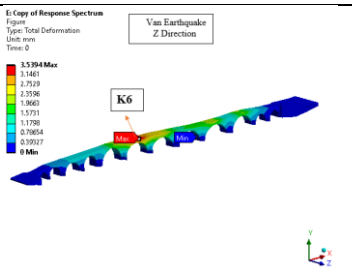
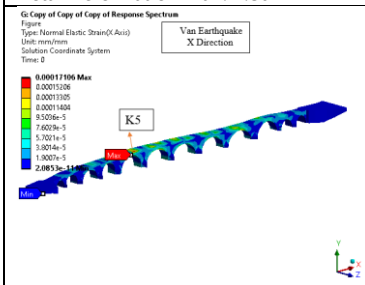
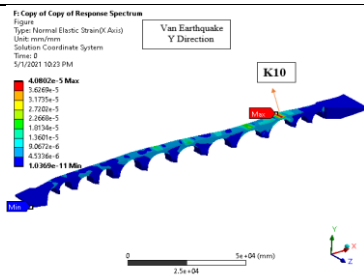
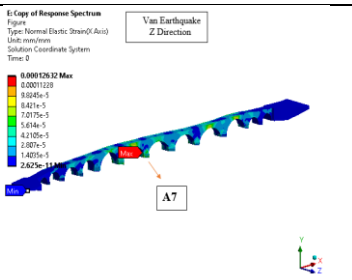
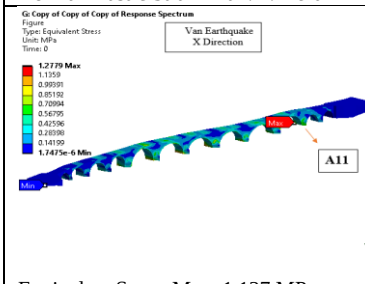
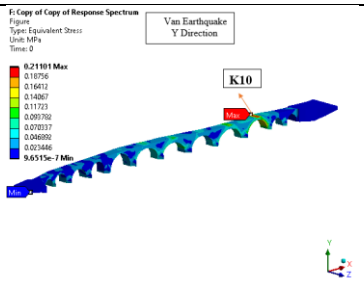
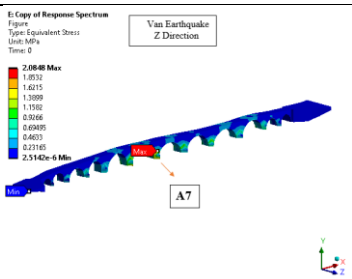
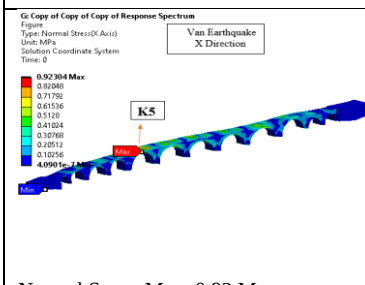
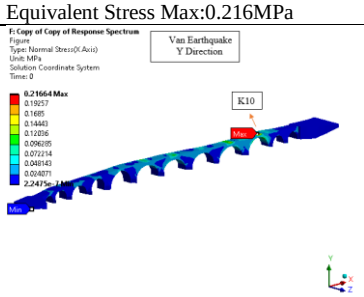
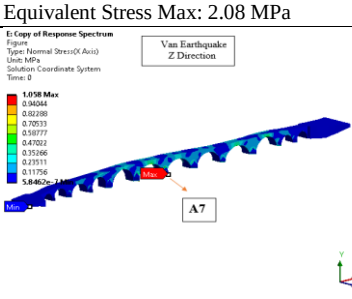
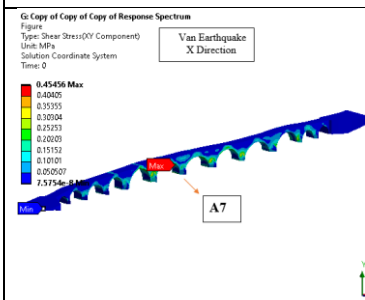
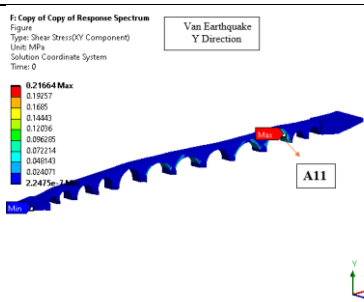
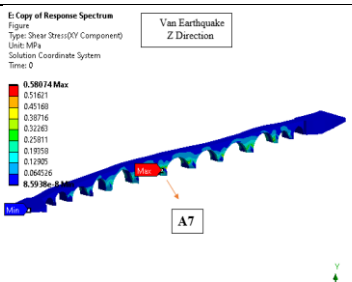
2011 VAN EARTHQUAKE		
X DİRECTİON	Y DİRECTİON	Z DİRECTİON
		
Total Deformation Max: 1.80 mm	Total Deformation Max: 0.38 mm	Total Deformation Max: 3.53 mm
		
Normal Elastic Strain Max: 1.71e-04 mm	Normal Elastic Strain Max: 4.08e-05 mm	Normal Elastic Strain Max: 1.26e-04 mm
		
Equivalent Stress Max: 1.127 MPa	Equivalent Stress Max:0.216MPa	Equivalent Stress Max: 2.08 MPa
		
Normal Stress Max: 0,92 Mpa	Normal Stress Max: 0.216 MPa	Normal Stress Max: 1,028 MPa
		
Shear Stress Max: 0,45 MPa	Shear Stress Max: 0,216 MPa	Shear Stress Max: 0.58 MPa

Figure 15. Imposed earthquake effects

BŞEÜ Fen Bilimleri Dergisi
8(1), 413-429, 2021

BSEU Journal of Science
https://doi.org/10.35193/bseufbd.949225

e-ISSN: 2458-7575 (https://dergipark.org.tr/tr/pub/bseufbd)

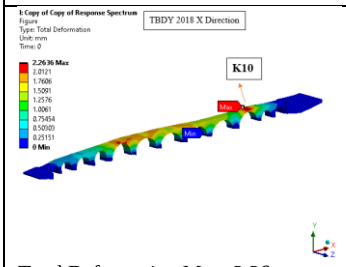
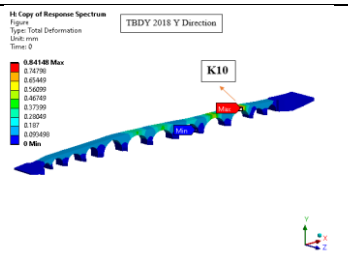
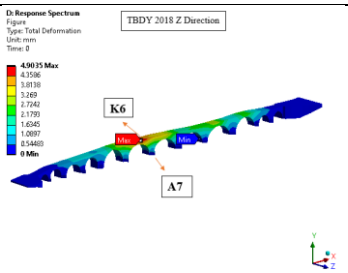
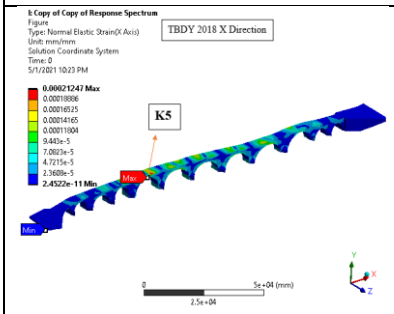
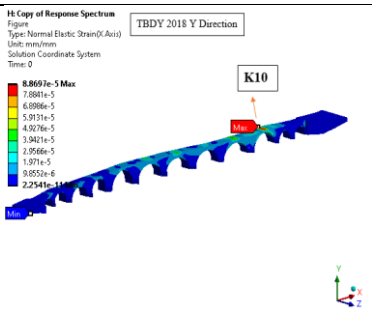
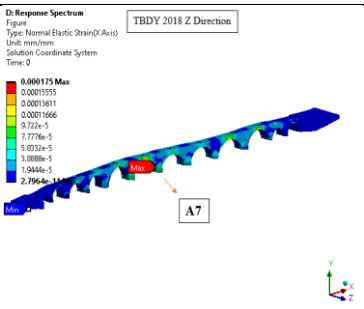
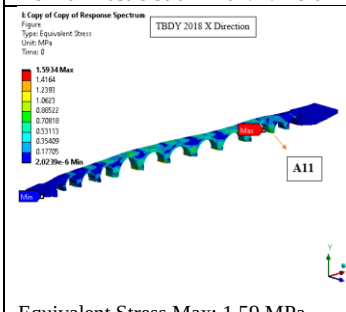
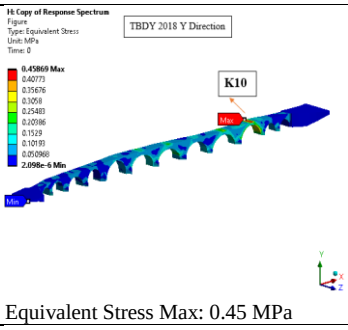
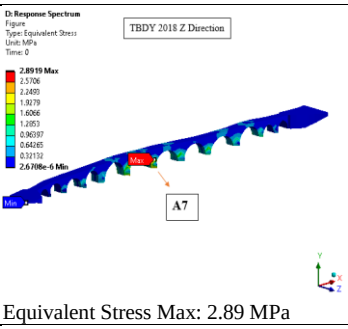
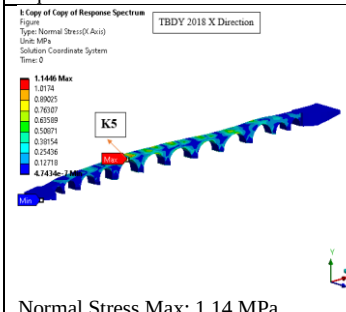
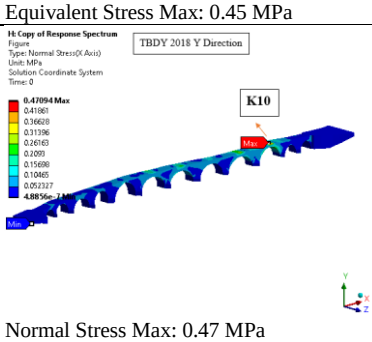
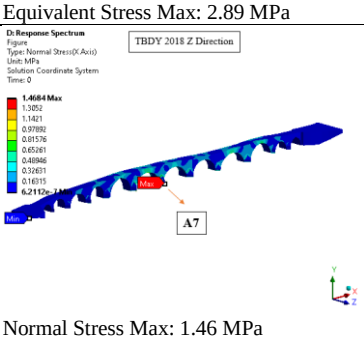
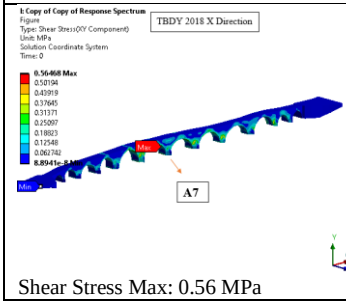
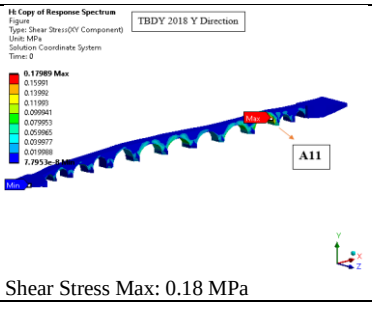
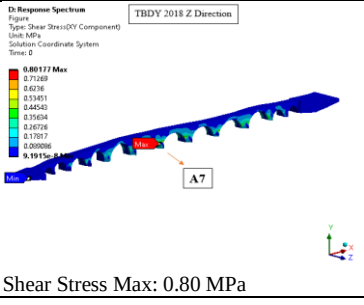
TBDY 2018		
X DİRECTİON	Y DİRECTİON	Z DİRECTİON
		
Total Deformation Max: 2.26 mm	Total Deformation Max: 0.84 mm	Total Deformation Max: 4.90 mm
		
Normal Elastic Strain Max: 2.12e-04 mm	Normal Elastic Strain Max: 8.86e-05 mm	Normal Elastic Strain Max: 1.75e-04 mm
		
Equivalent Stress Max: 1.59 MPa	Equivalent Stress Max: 0.45 MPa	Equivalent Stress Max: 2.89 MPa
		
Normal Stress Max: 1.14 MPa	Normal Stress Max: 0.47 MPa	Normal Stress Max: 1.46 MPa
		
Shear Stress Max: 0.56 MPa	Shear Stress Max: 0.18 MPa	Shear Stress Max: 0.80 MPa

Figure 15. (Continues)

C. Dead-Load, Vehicle and Hydrostatic Load Effects

As a result of dead, hydrostatic and vehicle loads, it was observed that the greatest deformation occurred in the K9 arch, which has the widest arch span of the bridge.

Although the direction of hydrostatic loading is different compared to other loads, the maximum stress occurred in the K9 arch and A11 pier of the bridge of the maximum deformation. It is thought that the curvature of the A11 pier of the bridge and the change in the height of the bridge in that region caused the tension at this point.

When the tensile and compressive stresses that occur in the structure under its own load are examined, it is seen that the part that is exposed to the highest tensile stress is in the upper part of the A7 pier.

As a result of vehicle loading, the tensile stress at the top of the A10 pier between the two wide-span arches of the bridge reached its maximum value.

As a result of the hydrostatic analysis, the maximum tensile stress occurred in the A pier of the bridge. The A11 pier of the bridge is located at the end of the curvature of the bridge in the longitudinal direction. This is thought to be the cause of stress. The results obtained in terms of loads are presented in Figure 16.

Considering the analysis results, the stress points of the structure were generally the same despite the different loadings

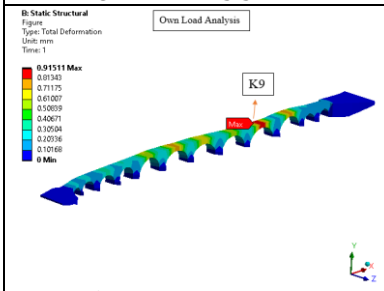
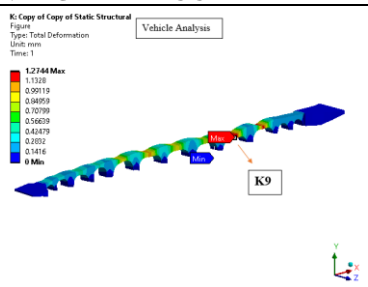
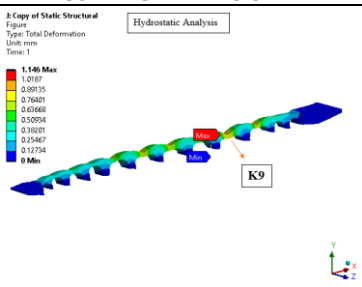
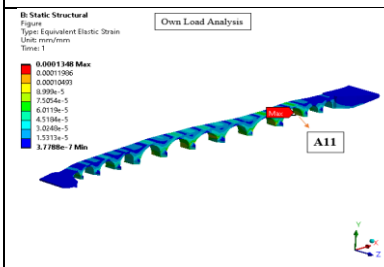
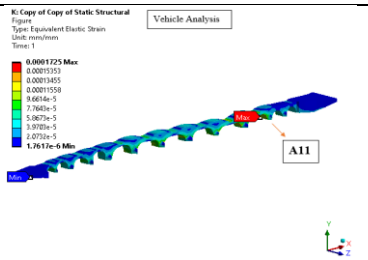
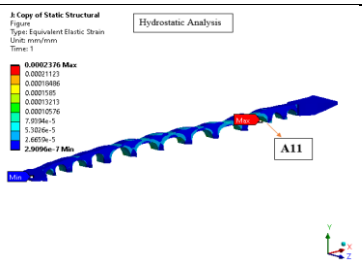
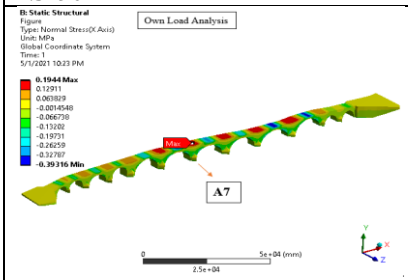
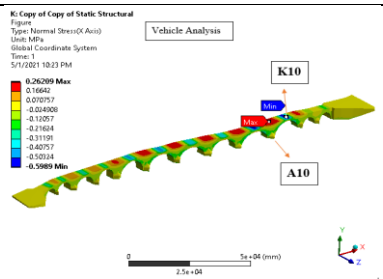
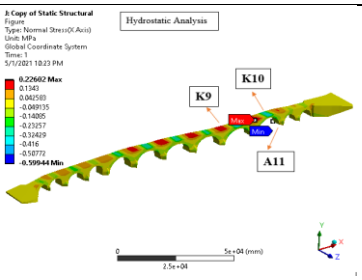
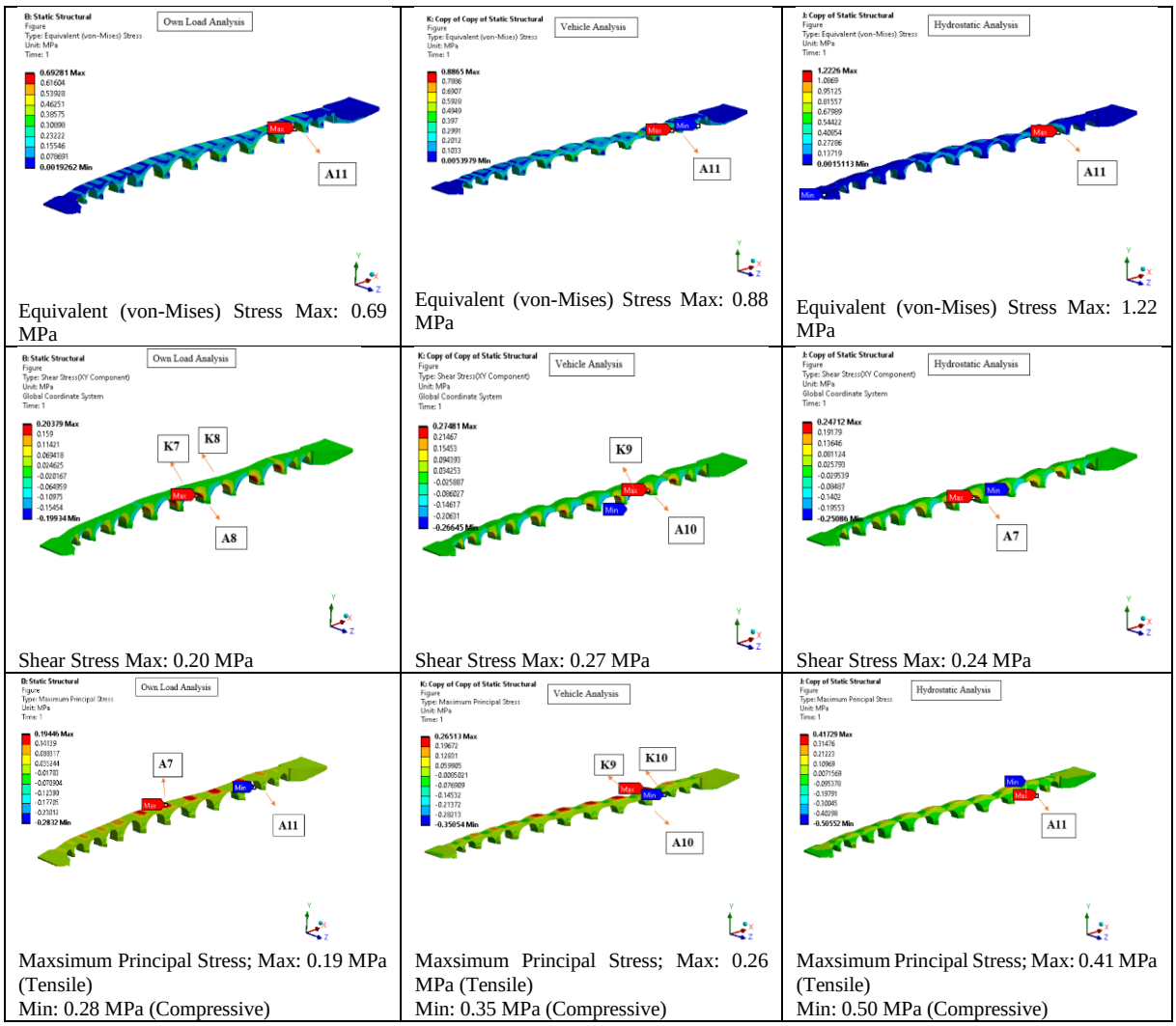
DEAD LOAD ANALYSIS	VEHICLE ANALYSIS	HYDROSTATIC ANALYSIS
 Total Deformation Max: 0.91 mm	 Total Deformation Max: 1.27 mm	 Total Deformation Max: 1.14 mm
 Equivalent Elastic Strain Max: 1.34e-04 mm	 Equivalent Elastic Strain Max: 1.72e-04 mm	 Equivalent Elastic Strain Max: 2.37e-04 mm
 Normal Stress Max(+): 0.19 MPa Max (-): 0.39 MPa	 Normal Stress Max(+): 0.26 MPa Max (-): 0.59 MPa	 Normal Stress Max(+): 0.22 MPa Max (-): 0.59 MPa

Figure 16. Imposed load results



Equivalent (von-Mises) Stress Max: 0.69 MPa

Equivalent (von-Mises) Stress Max: 0.88 MPa

Equivalent (von-Mises) Stress Max: 1.22 MPa

Shear Stress Max: 0.20 MPa

Shear Stress Max: 0.27 MPa

Shear Stress Max: 0.24 MPa

Maxsimum Principal Stress; Max: 0.19 MPa (Tensile)
Min: 0.28 MPa (Compressive)

Maxsimum Principal Stress; Max: 0.26 MPa (Tensile)
Min: 0.35 MPa (Compressive)

Maxsimum Principal Stress; Max: 0.41 MPa (Tensile)
Min: 0.50 MPa (Compressive)

Figure 16. (Continues)

V. CONCLUSION

As a result of the analysis, the stress points of the Mus Historical Murat Bridge were determined.

It has been observed that a wide arch span will cause an increase in the stresses that will occur in this region. For this study, it was monitored that the K9 and K10 arches, which have the most span, were exposed to more stress.

As a result of the modal analysis, it was observed that the first natural frequency of the bridge was formed in the K6 arch and this arch was one of the highest of the structure. As a result of the earthquake loads in the X and Z direction, it was observed that the maximum shear stresses occurred at the A7 leg located in the middle of the bridge. As a consequence of the earthquake effect applied to the bridge in the vertical direction (Y direction), the stresses concentrated in the curved area (K10, A11) on the bridge.

As a result of the hydrostatic analysis, it is seen that the water created the highest stress in the A11 pier and K10 arch of the bridge. The historical structure is not straight in the longitudinal direction in this region. The highest stress in loads other than earthquakes occurred aftermath of hydrostatic analysis. Deformations most commonly occurred in the K9 arch, which has the largest width of the bridge. The highest compressive stress occurred in the A11 piers of the bridge.

As a result of earthquake and loading effects in different directions, it was observed that the loads imposed on the bridge in the Z direction caused the bridge to be exposed to more stress.

The greatest stresses in the bridge were obtained as a result of the earthquake analysis, which were applied in the Z direction.

REFERENCES

[1] Çulpan, C. (2002) Türk Taş Köprüleri; Ortaçağdan Osmanlı Devri Sonuna Kadar, Türk Tarih Kurumu, Ankara.

[2] Genç, A. F. (2015) Tarihi Köprülerin Yapısal Davranışına Restorasyon Çalışmalarının Etkisi, Yüksek Lisans Tezi, Karadeniz Teknik Üniversitesi, Fen Bilimleri Enstitüsü, Trabzon

[3] Tunç, G. & Kulağuz, B. N. (1996) Muş ve Çevresindeki Türk Mimari Eserleri, YüzüncüYıl Üniversitesi, Sosyal Bilimler Enstitüsü Sanat Tarihi Anabilim Dalı Yayınlanmamış Yüksek Lisans Tezi, 85.

[4] Işık, E., Aydin, M. C. & Ülker, M. (2016) Performance Evaluation of a Historical Tomb and Seismicity of the Region. *Bitlis Eren University Journal of Science and Technology*, 6, 59–65.

[5] Gönen, H., Doğan, M., Karacasu, M., Ozbasaran, H. & Gökdemir, H. (2013). Refrofit tarihi murat yığma kemer köprüsünde yapısal başarısızlıklar, *Engineering Failure Analysis*. 35, 334-342 https://doi.org/10.1016/j.engfailanal.2013.02.024

[6] Karaton, M., Aksoy, H. S., Say, E. & Calay, Y. (2017) Nonlinear seismic performance of a 12th century historical masonry bridge under different earthquake levels. *Engineering Failure Analysis*, 79, 408–421. doi: 10.1016/j.engfailanal.2017.05.017.

[7] Stavroulaki, M. E., Riveiro, B., Drosopoulos, G. A., Solla, M., Koutsianitis, P. & Stavroulakis, G. E. (2016) Advances in Engineering Software Modelling and strength evaluation of masonry bridges using terrestrial photogrammetry and finite elements, *Advances in Engineering Software*. 101, 136–148. doi: 10.1016/j.advengsoft.2015.12.007.

[8] Valente, M. & Milani, G. (2016) Seismic assessment of historical masonry towers by means of simplified approaches and standard FEM. *Construction and Building Materials*, 108, 74–104. doi: 10.1016/j.conbuildmat.2016.01.025.

[9] Aguilar, R., Noel, M. F. & Ramos, L. F. (2019) Integration of reverse engineering and non-linear numerical analysis for the seismic assessment of historical adobe buildings. *Automation in Construction*. 98, 1–15. doi: 10.1016/j.autcon.2018.11.010.

[10] Betti, M. & Galano, L. (2012) Seismic Analysis of Historic Masonry Buildings: The Vicarious Palace in Pescia (Italy). *Buildings*, 63–82. doi: 10.3390/buildings2020063.

[11] Pachón, P., Castro, R., García-macías, E., Compan, V. & Puertas, E. (2018) E. Torroja's bridge: Tailored experimental setup for SHM of a historical bridge with a reduced number of sensors. *Engineering Structures*. 162, 11–21. doi: 10.1016/j.engstruct.2018.02.035.

[12] Ercan, E. (2018) Assessing the impact of retrofitting on structural safety in historical buildings via ambient vibration tests. *Construction and Building Materials*, 164, 337–349. doi: 10.1016/j.conbuildmat.2017.12.154.

[13] Sarhosis, V., Garrity, S. W. & Sheng, Y. (2015) Influence of brick – mortar interface on the mechanical behaviour of low bond strength masonry brickwork lintels. *Engineering Structures*. 88, 1–11. doi: 10.1016/j.engstruct.2014.12.014.

[14] ANSYS. (2019). Swanson Analysis System, U.S.A.

[15] Simos, N., Manos, G. C. & Kozikopoulos, E. (2018) Near- and far-field earthquake damage study of the Konitsa stone arch bridge. *Engineering Structures*, 177, 256-267. https://doi.org/10.1016/j.engstruct.2018.09.072

[16] Chen, X., Qi, X. & Xu, Z. (2019). Determination of weathered degree and mechanical properties of stone relics with ultrasonic CT: A case study of an ancient stone bridge in China, *Journal of Cultural Heritage*, 42, 131–138. https://doi.org/10.1016/j.culher.2019.08.007

[17] Castro, A.B., Sancez-Aparicio, L.J., Ramos L.F., Sena-Cruz, C. & Gonzalez-Aguilera, D., (2018). Integrating geomatic approaches, Operational Modal Analysis, advanced numerical and updating methods to assess the current security conditions of the historic Bôco Bridge, *Construction and Building Metarials*, 185, 961-984. https://doi.org/10.1016/j.conbuildmat.2017.10.084

[18] Tanrıverdi, M. (2019). Geçmişten Günümüze Tarihi Köprüler, Yüksek Lisans Tezi, Harran Üniversitesi, Fen Bilimleri Enstitüsü, Şanlıurfa.

[19] Arede, A., Almeida, C., Costa, C. & Costa, A., (2019). In-situ and lab tests for mechanical characterization of stone masonry historical structures, *Construction and Building Metarials*, 220, 503-515 https://doi.org/10.1016/j.conbuildmat.2019.06.039
[20] Türkiye Deprem Tehlike Haritası, TBDY 2018, https://deprem.afad.gov.tr/deprem-tehlike-haritasi (Axess: 22.04.2020)
[21] Yeşilbaş, E. (2016). Muş Murat Köprüsü Sanat Tarihi Raporu
[22] Öztürk, S. (2005). Muş Murat Köprüsü Rölöve-Restitüsyon ve Restorasyon Projelerine ait Çalışma Dostyası
[23] Ural, A. (2005). Tarihî Kemer Köprülerin Sonlu Eleman Metoduyla Analizi. Deprem Sempozyumu, Mart, Kocaeli, Türkiye, 408-413.
[24] Ural, A. (2017). Muş Murat Köprüsü Yapısal Analiz ve Değerlendirme Raporu
[25] Akan, E. A. & Özen, Ö., (2005) Bursa Yeşil Türbenin Sonlu Elemanlar Yöntemi ile Deprem Analizi, Deprem Sempozyomu, Mart, Kocaeli, Türkiye, 758-762.
[26] Fuat, A., Ergün, M., Günaydin, M. & Can, A. (2019). Dynamic analyses of experimentally-updated FE model of historical masonry clock towers using site-specific seismic characteristics and scaling parameters according to the 2018 Turkey building earthquake code. *Engineering Failure Analysis*. 105, 402–426. doi: 10.1016/j.engfailanal.2019.06.054.
[27] Terzi, V. G. & Ignatakis, C. E. (2018). Nonlinear finite element analyses for the restoration study of Xana, Greece. *Engineering Structures*. 167, 96–107. doi: 10.1016/j.engstruct.2018.04.034.
[28] Güney, D. (2011) 23 Ekim 2011 Van Depremi Teknik İnceleme Raporu, Yıldız Teknik Üniversitesi, İstanbul
[29] Alkan, A., Baykan, O., Atalay, A., Baykan, N. & Öziş, Ü. (2011). Su Yapıları Olarak Anadolu'daki Taş Köprüler, 2. Su Yapıları Sempozyumu 16-18 Eylül 2011